HEFAT2007
5th International Conference on Heat Transfer, Fluid Mechanics and Thermodynamics
Sun City, South Africa
Paper number: KH1

EXPERIMENTAL AND NUMERICAL STUDIES ON VORTICAL STRUCTURE AND TEMPERATURE FIELD IN A BLUFF-BODY BURNER

Kawahara H.* and Nishimura T.
*Author for correspondence
Shipping of Technology Department,
Oshima National College of Maritime Technology,
1091-1, Komatsu, Suo-oshima-cho, Oshima-gun, Yamaguchi, 742-2193
Japan,
E-mail: kawahara@s.oshima-k.ac.jp

ABSTRACT

Vortical and thermal structures of non-premixed propane flame in a bluff-body burner are studied experimentally and numerically in the transition from laminar to turbulent flow. In particular, we focus attention on the effect of annular air flow on the flame. The annular air flow promotes development of a shear layer vortex street in the central fuel jet and lends to change in the direction of rotation of the vortex. These features are supported by the numerical simulation. The agreement of experimental and numerical vortex frequencies is satisfactory. The fluctuation in temperature corresponds well to the vortex dynamics, and there is a peak in rms temperature inside and outside the flame, respectively.

INTRODUCTION

Non-premixed flame stabilized by a bluff-body combustor, such as occurs when a central fuel jet issues into a surrounding annular air flow, is often used industrially. Such bluff-body combustors provide good flame stabilization as well as easy control of combustion.

There have been experimental studies on non-premixed flames for several fuels. Roquemore et al. [1] introduced a two-dimensional sheet-lighting technique coupled with a fast chemically reacting system to visualize the turbulent mixing and the vortex shedding processes of a bluff-body combustor for C_3H_8. Lin and Tankin [2] employed this technique and determined the effect of burner design and flow conditions on fuel jet penetration at low Reynolds numbers. Furthermore, Chin and Tankin [3] and Nishimura and Takemori [4] measured vortical shedding frequency using a flow visualization technique in a two-dimensional slot burner and cylindrical shaped burners, respectively. Huang and Lin [5] studied the flame behaviour and the time-averaged thermal structure for various C_3H_8 and air flows. Schefer et al. [6] and Namazian et al. [7] performed velocity and concentration measurements using laser Doppler velocimetry and a combined Raman scattering and laser-induced fluorescence imaging in turbulent flow for CH_4. Lee and Onuma [8] also measured velocity, temperature and chemical species in turbulent flow for H_2 in order to compare with numerical simulation.

Although they emphasized the importance of vortical structures in bluff-body burners, the relationship between the vortical and thermal structures under unsteady vortical motion has not been understood fully in the experimental studies. While, more recently, direct numerical simulation have been performed in the transitional flow regime for jet diffusion flames to capture the temporal and spatial development of vortical and thermal structures, i.e., Katta and Roquemore [9], Yamashita et al. [10]. Such a simulation will be extended to bluff-body burners in the near future. However, there have been few studies providing time-dependent experimental data to test and refine mathematical modelling. These aspects have motivated the present investigation. Vortical and thermal structures in a bluff-body burner are studied experimentally and numerically in the transition from laminar to turbulent flow as a necessary initial step in a more realistic situation involving fully turbulent flow. In the present study, we focus attention on the effect of annular air flow on the flame, and it is expected that the fuel jet in the transition regime is responsive to the annular air flow.

EXPERIMENTAL APPARATUS AND PROCEDURE

The bluff-body, vertical, unducted combustor used here consisted of a fuel nozzle located concentric to an annular region where air flowed, as shown in Figure 1. Commercial-grade propane was employed as the fuel gas. The diameters of the fuel nozzle D_j, the inner annulus D_i and the outer annulus do were 10mm, 42mm and 56mm, respectively. One of the objectives of the present study is to examine the effect of the annular air velocity, listed in Table 1. It should be noted that the jet at this fuel velocity belongs to the transition regime, in the absence of the annular air flow.

The relationship between vortical structure and temperature field was examined by flow visualizations, velocity and

temperature measurements. A schematic diagram of the experimental set-up is shown in Figure 2. The vortical structure was visualized by combination of the shadowgraph method and high-speed camera. The motion pictures were analyzed with an image processor. The mean velocity is measured by a LDV system. A fine wire thermocouple compensated for the effect of thermal inertia was employed to examine the characteristics of temperature fluctuation, i.e., Pt-Pt/Rh 13%, 50 μ m in diameter. No coatings were applied to the thermocouple to inhibit catalytic activity because of the increase in the time constant,

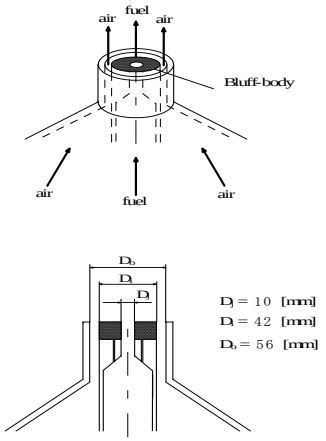

Figure 1 Bluff-body burner

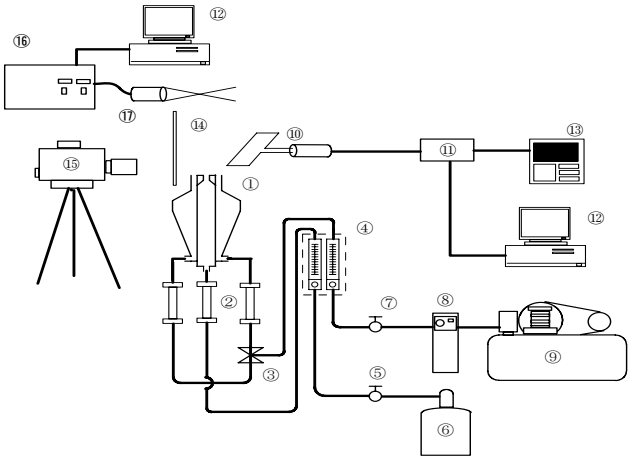

Figure 2 Experimental apparatus

Table 1 Test matrix

Case	Central fuel jet		Annular air flow		u_j/u_a
	u_j (m/s)	Re_j	u_a (m/s)	Re_a	
A	0.84	1957	0.0	0.0	0.0
B	0.84	1957	0.62	563	0.738
C	0.84	1957	1.24	1126	1.476

43ms. The thermocouple with the compensator is presumed to follow temperature fluctuations of 2kHz. The dominant temperature fluctuation is less than 0.5kHz in this experiment. The information on the flow visualization and temperature measurement was simultaneously monitored to make clear the interrelation of these data.

NUMERICAL MODEL

The axial symmetry of the flow is satisfied from conventional experimental result in such flow field. Therefore, computation model was assumed the axially symmetry. The present computational domain is shown in Figure 3. The flow is time-dependent and two-dimensional. The axisymmetric coordinate system is taken such that x is the streamwise direction, r is the radial and the origin is the center of the fuel injection with a diameter of 1.0d, and the thickness of the bluff-body was made with 1.5d in order to be correspondent to burner nozzle used by the experiment. In addition, the annulus jet of air flow had a 0.7d. u and v represent the streamwise and transverse velocity, respectively, and z is the coupling function. The boundary conditions for u , v and z for the combusting flow are described in the figure. The conservation equations for mass and momentum are given in the following forms.

$$\frac{\partial \rho}{\partial t}+\frac{\partial \rho u}{\partial x}+\frac{1}{r}\cdot\frac{\partial (r\rho v)}{\partial r}=0 \tag{1}$$

$$\begin{aligned}&\frac{\partial(\rho u)}{\partial t}+\frac{\partial(\rho uv)}{\partial x}+\frac{\partial(\rho uv)}{\partial r}=\frac{\partial}{\partial x}\left(\mu\frac{\partial u}{\partial x}\right)+\frac{\partial}{\partial r}\left(\mu\frac{\partial u}{\partial r}\right)\\&-\frac{\rho uv}{r}+\frac{\mu}{r}\frac{\partial u}{\partial r}-\frac{\partial p}{\partial x}+(\rho_a-\rho)g+\frac{\partial}{\partial x}\left(\mu\frac{\partial u}{\partial x}\right)+\frac{\partial}{\partial r}\left(\mu\frac{\partial v}{\partial x}\right)\\&+\frac{\mu}{r}\frac{\partial v}{\partial x}-\frac{2}{3}\left\{\frac{\partial}{\partial x}\left(\mu\frac{\partial u}{\partial x}\right)+\frac{\partial}{\partial x}\left(\mu\frac{\partial v}{\partial r}\right)+\frac{\partial}{\partial x}\left(\mu\frac{v}{r}\right)\right\}\end{aligned} \tag{2}$$

$$\begin{aligned}&\frac{\partial(\rho v)}{\partial t}+\frac{\partial(\rho uv)}{\partial x}+\frac{\partial(\rho uv)}{\partial r}=\frac{\partial}{\partial x}\left(\mu\frac{\partial v}{\partial x}\right)+\frac{\partial}{\partial r}\left(\mu\frac{\partial v}{\partial r}\right)\\&-\frac{\rho uv}{r}+\frac{\mu}{r}\frac{\partial v}{\partial r}-\frac{\partial p}{\partial r}+\frac{\partial}{\partial x}\left(\mu\frac{\partial u}{\partial r}\right)+\frac{\partial}{\partial r}\left(\mu\frac{\partial v}{\partial r}\right)\\&+\frac{\mu}{r}\frac{\partial v}{\partial r}-2\mu\frac{v}{r^2}-\frac{2}{3}\left\{\frac{\partial}{\partial r}\left(\mu\frac{\partial u}{\partial x}\right)+\frac{\partial}{\partial r}\left(\mu\frac{\partial v}{\partial r}\right)+\frac{\partial}{\partial r}\left(\mu\frac{v}{r}\right)\right\}\end{aligned} \tag{3}$$

where t and ρ are the time and density, suffix a denotes environment condition. Density is related to pressure p , temperature T and mass fraction Y_i through the following state equation

$$p=\rho\cdot R\cdot T\sum_{i=1}^{4}\left(Y_i/m_i\right) \tag{4}$$

where m_i is the molecular weight of species I and R is the universal gas constant. The problem is further simplified by adopting the following coupling function z , i.e., Shavb-Zeldvich formulation:

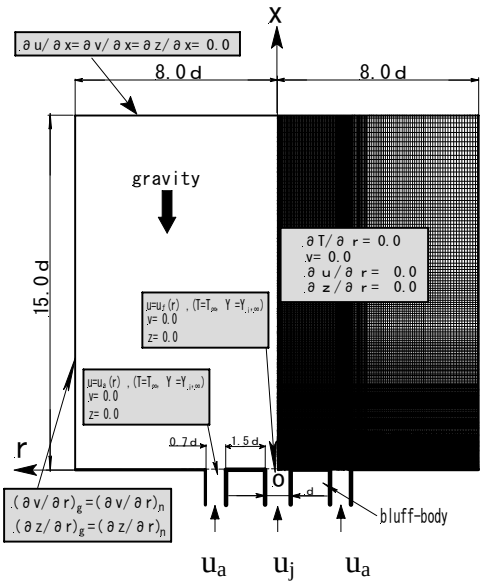

Figure 3 Analytical domain and boundary conditions

$$z = \frac{Y_I - Y_{I,\infty}}{Y_{I,O} - Y_{I,\infty}} = \frac{Y - Y_\infty}{Y_O - Y_\infty} = \frac{h - h_\infty}{h_O - h_\infty} \tag{5}$$

where Y is given by

$$\mathrm{Y} = \left(\mathrm{Y_F} / m_F \cdot \nu_F\right) - \left(Y_O / m_O \cdot \nu_O\right) \tag{6}$$

and h is the sum of the thermal and chemical enthalpies. Suffix o denotes the value for the injected fuel, while ∞ denotes the value for the co-flowing air stream. The energy conservation equation and the mass conservation equations for each species reduce to the following equation for z:

$$\frac{\partial(\rho z)}{\partial t} + \frac{\partial(\rho u z)}{\partial x} + \frac{\partial(\rho v z)}{\partial r} = \frac{\partial}{\partial x}\left(\rho D \frac{\partial z}{\partial x}\right) + \frac{\partial}{\partial r}\left(\rho D \frac{\partial z}{\partial r}\right) - \frac{\rho v z}{r} + \frac{\rho D}{r}\frac{\partial z}{\partial r} \tag{7}$$

The flame surface is located at the position where z becomes equal to z_f, given by the equation:

$$z_f = \left(Y_{O,\infty} / j\right) / \left(1 + \left(Y_{O,\infty} / j\right)\right) \tag{8}$$

where $j = m_o \nu_o / m_F \nu_F$, i.e., mass of oxygen required to burn unit mass of fuel to attain complete combustion. The flame surface divides the whole region into two regions, i.e., fuel region inside the flame and air region outside the flame. The mass fractions and temperature in the respective regions can be written as follows for the when $Y_{I,o} = 0$

Fuel region $\left(1 \ge z \ge z_f\right)$

$$Y_I = Y_{I,\infty}(1 - z) T = T_\infty + \left(T_O - T_\infty\right) z + \left(q_O / m_F \nu_F c_P\right) j^{-1} \cdot Y_{O,\infty}(1 - z) \tag{9}$$

Air region $\left(z_f \ge z \ge 0\right)$

$$T = T_\infty + \left(T_o - T_\infty\right) z + \left(q_o / m_F \nu_F c_p\right) z \tag{10}$$

In the present study, we shall adopt the following assumptions.

*The mixture undergoes an overall one-step irreversible reaction.

*The reaction rate is infinitely fast and the reaction is concentrated within infinitesimally thin zone in the surface.

*The mixture behaves like an ideal gas.

*The Soret and Dufour effect, as well as the pressure diffusion, can be neglected.

*Specific heat at constant pressure of the mixture is constant.

*The Lewis number is equal to unity.

*Viscosity coefficient and diffusion coefficient depend on temperature.

*In the energy equation viscous dissipation can be neglected.

The numerical calculation was performed by the finite-difference method [10]. The scheme adopted here was the SIMPLE method. The time differential and convective terms in the governing equations are treated with the implicit Euler scheme and QUICK scheme, respectively. The computational domain is $0 \le x \le 15.0d$ and $0 \le r \le 8.0d$. The grid number are 121×261 non-uniform grid systems.

RESULTS AND DISCUSSION

Vortical Structures

The flame formed by a bluff-body burner is formed by a fuel flow from the center of a concentric double pipe and an air flow emitted by an annulus.

Figure 4 shows a direct photograph of a flame under the conditions shown in Table 1. In case A, which involves the fuel jet alone, the flame attaches to the inside of the bluff body, while in case B, where an air flow is flowing, the flame attaches to the outside of the bluff body. In addition, comparison of the shape of the flame surface indicates that the flame surface in case A develops downstream with substantial bulges while in case B it is relatively smooth and appears as bands in the horizontal direction. In case C, in contrast, uneven folds are observed in the vertical direction.

Figure 5 shows the streakline distribution determined by numerical calculations and shadowgraph photographs corresponding to Figure 4. According to shadowgraph photographs, shear vortices are formed in all of the fuel flows, and the position at which rotation of shear vortices from

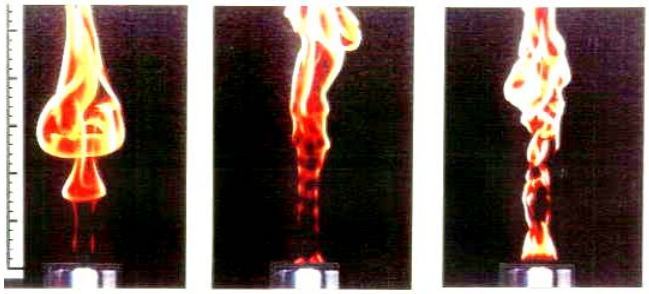

case A case B case C

Figure 4 Direct pictures for cases A, B and C

Shadowgraph images

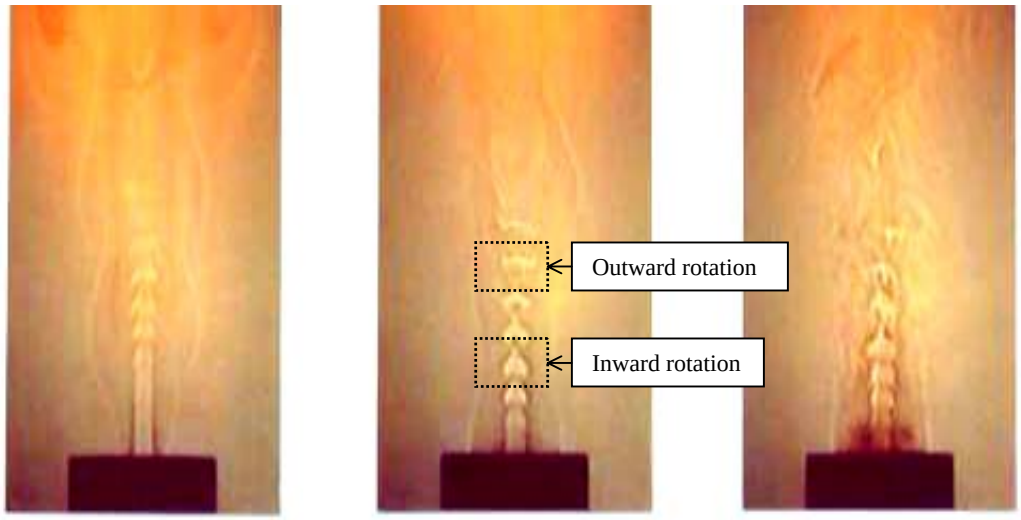

Computational visualization

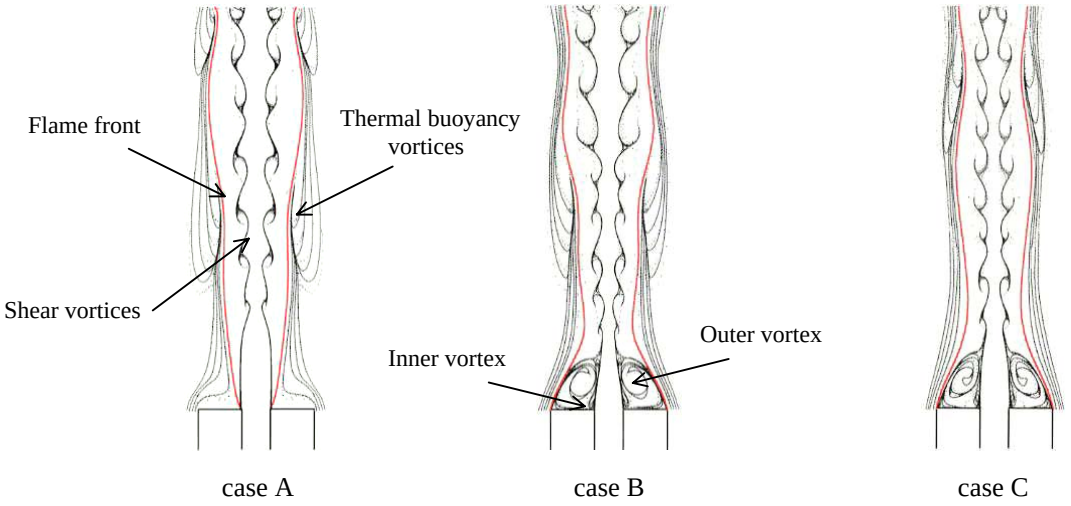

Figure 5 Shadowgraph images and numerical streakline patterns for cases A, B and C

outward to inward due to the effects of the air flow shifts upstream. As became apparent in case C, shear vortices are disrupted downstream, and air flow through the flame largely affects fuel flow. The existence of a circulation flow and reversal of shear vortices corresponded well with calculated results, but the vortex breakdown in case C could not be reproduced. However, focusing on the area outside the flame indicated that vortices due to thermal buoyancy weakened due to the air flow.

Figure 6 shows the relationship between the frequencies of shear vortices in fuel and air flow. The calculated frequencies were determined from changes over time in the velocity components along the x axis at r/d = 0.5 and x/d = 5.0. In addition, in experiments these were measured based on shadowgraph images from a high-speed video camera. The St_f number, i.e. the dimensionless frequency, decreased due to an increase in air flow, and calculations and experiments roughly matched.

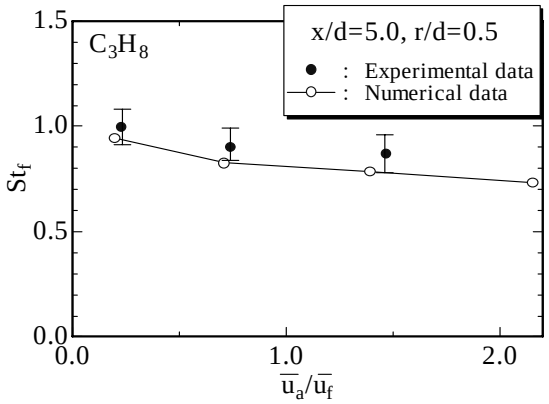

Figure 6 Strouhal number vs. u_a/u_f for experimental and numerical data

Next, Figure 7 shows the time-averaged velocity distribution at x/d＝7.0, which was used to examine the reversal of shear vortices. In experiments, this was measured by LDV. In case B, experiments and calculations agreed, but they did not do so in case C. This is because disruptions such as vortex breakdown could not be reproduced, as was mentioned previously. With regard to velocity in the fuel flow, however, velocity at the flame rather than in the center of the fuel increased, and the velocity gradient directly above the bluff body reversed. As became apparent, reversal of shear vortices depended on the velocity gradient, and its effects increased due to an increase in the air flow.

Although the above results revealed some inconsistencies between calculations and experiments, aspects such as the frequencies of shear vortices agreed, and the essential structure of vortices in the bluff-body burner can be ascertained.

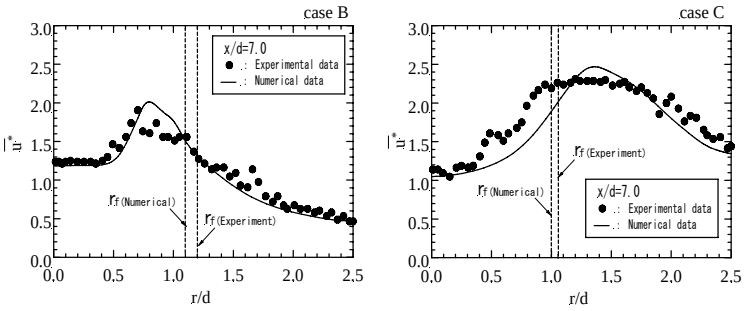

case B case C

Figure 7 Time-averaged axial velocity profiles at x/d=7.0 for cases B and C

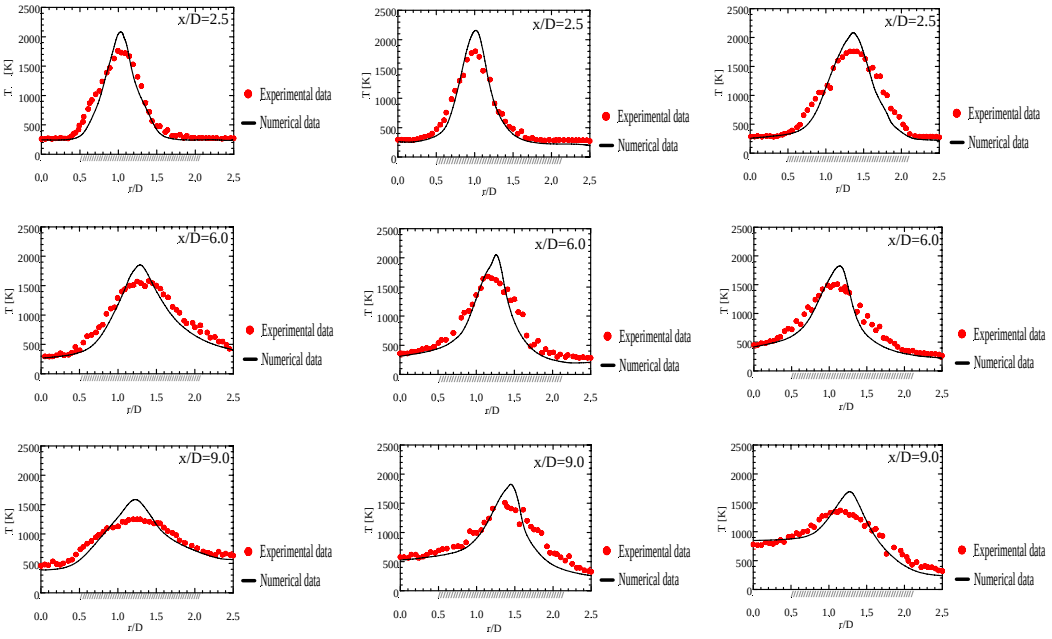

case A case B case C

Figure 8 Radial profiles of time-averaged temperatures for cases A, B and C

Temperature field

Figure 8 shows the temperature distribution in a horizontal cross-section at 3 points, which was used for quantitative comparison. Disparities in calculations and experiments were noted in the vicinity of the maximum temperature, indicating the reaction zone, but temperatures at other locations agreed in all of the cases. With regard to disparities in the vicinity of the maximum temperature, radiation corrections were made in experiments while the effects of radiation were ignored in calculations.

Last, RMS values of temperature fluctuations were divided by the time-averaged temperature and made dimensionless; the fluctuation intensity map obtained is shown in Figure 9. In the figure, the time-averaged position of the flame is also shown as a solid line. Qualitatively, calculations corresponded well with experiments, though absolute values for fluctuation intensity were larger in calculations than in experiments.

The cause lies in the results of visualization: in calculated results, as mentioned previously, the macroscopic dynamic behaviour of vortices can be accurately ascertained, but the microscopic behaviour of vortices cannot be ascertained because of the level of precision of these calculations, and these fluctuations in behaviour of vortices appear more marked in experiments. Next, observation of the fluctuation intensity in each case indicated that in case A a strong peak of the same extent appeared outside and inside the flame in the vicinity of x/d=7.0 in experiments and x/d=8.5 in calculations. As indicated by frequency analysis [4], both were fluctuations produced by vortices due to thermal buoyancy; as became apparent, via the flame front these vortices caused strong fluctuations at the fuel jet as well. In contrast, in case B a peak in strong fluctuations outside the flame existed, but inside the flame fluctuations weakened. The peak in fluctuations outside the flame was similar to that in case A. Vortices due to thermal buoyancy had

an effect, but the peak inside the flame was due to the interaction of vortices due to thermal buoyancy and shear vortices. In case C, a peak of the same extent outside and inside the flame also appeared. This is due to the effects of the air flow flowing outside the flame. In addition, this fluctuating zone was more limited in calculated results than in experimental results; this is due to the effects of vortex breakdown observed in the downstream region in experiments. Based on the above results, the peak in temperature fluctuations corresponds to the behaviour of vortices due to thermal buoyancy and shear vortices.

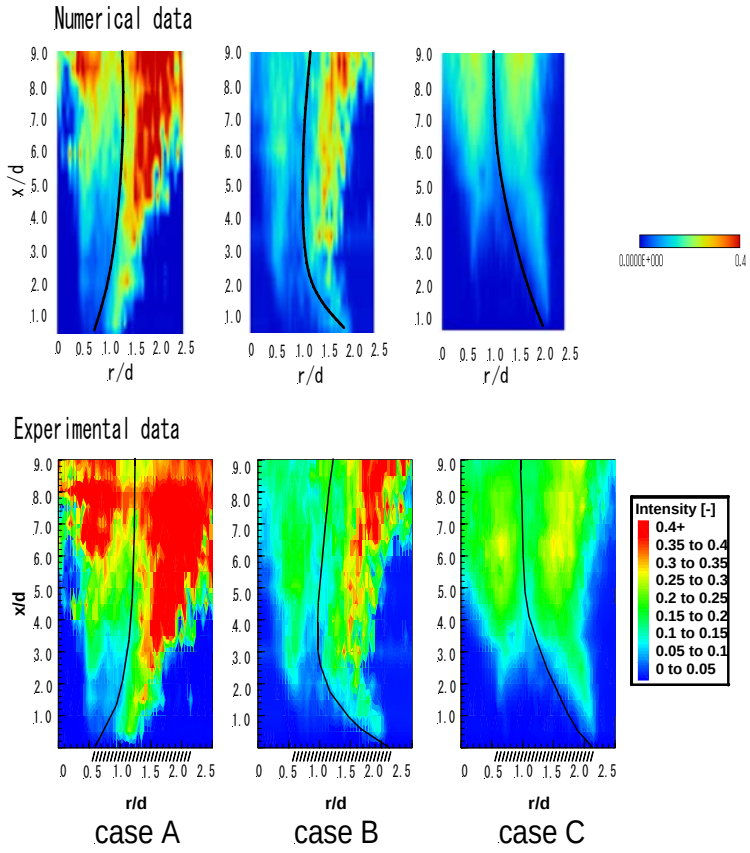

Figure 9 Contourlines of RMS temperature for cases A, B and C

Therefore, it was confirmed that the numerical simulation on combustion field in the bluff-body burner aft was catching actual phenomenon in the range of this experimental condition. Concretely, it was proven that the interaction between large vortical structure and flame in the combustion field was effective even in combustion model and two-dimensional calculation assumed in this investigation. However, there is a limit of the two-dimensional calculation with that the air flow is made to increase like case C, since the flow field becomes turbulent flow.

CONCLUSION

This work conducted a numerical study of the relationship between the flame and vortical structures in an axisymmetric bluff-body burner, as is widely used in practical combustion fields. Given the validity of these calculations with respect to experimental results, the following findings were obtained:

(1) As regards a combustion field with a circulation flow in the transition zone, the calculated results roughly matched the flow structure as indicated by experimental results.
(2) In a combustion field with a circulation flow where an air flow is flowing, a stable recirculation zone is formed in the vicinity of the nozzle outlet, and this encourages the development of shear vortices in the fuel jet.
(3) The position at which shear vortices in the fuel jet reverse shifts upstream with an increase in the Re_a number of the air.
(4) Vortices due to thermal buoyancy and shear vortices each induce temperature fluctuations, and a peak in fluctuation intensity appears on both sides of the flame front. Within the range of conditions in this study, vortices due to thermal buoyancy had a more marked effect on temperature fluctuations than shear vortices.

REFERENCES

[1] Roquemore, W.M., Tankin, R.S., Chiu, H.H. and Lottes, S. A., A study of a Bluff-body combusting using laser sheet lighting, *Experimental Fluids, 4*, 1986, pp. 205-213

[2] Li, X. and Tankin, R.S., A study of cold and combusting flow around Bluff-body combustors, *Combustion Science and Technology*, Vol. 52, 1987, pp. 173-206

[3] Chin, L.P. and Tankin, R.S., Vortical structures in a 2-d vertical Bluff-body burner, *Combustion Science and Technology*, Vol. 80, 1991, pp. 207-229

[4] Nishimura, T. and Takemori, I., Vortical structures of combusting flow around Bluff-body burner, *Proceedings of the 7th International Conference on Flow Visualization*, Seattle, 512-517, July 1995.

[5] Hung, R.F. and Lin, C.L., Characteristic modes and thermal structures of non-premixed circular-disc stabilized flames, *Combustion Science and Technology*, Vol. 100, 1994, pp. 123-139

[6] Schefer, R.W., Namazian, M. and Kelly, J., Velocity measurement in a turbulent non-premixed Bluff-body stabilized flame, *Combustion Science and Technology*, Vol. 56, 1987, pp. 101-138

[7] Namazian, M., Kelly, J., Schefer, R.W., Johnston, S.C. and Long, M.B., Non-premixed Bluff-body burner flow and flame imaging study, *Experimental Fluids*, Vol. 8, 1989, pp. 216-228

[8] Lee, C.E. and Onuma, Y., Experimental study of turbulent diffusion flames stabilized on a Bluff-body – 1st Report, Flame structure, *Trans JSME Ser.B*, Vol. 57, 1991, pp. 4266-4271

[9] Katta, V.R. and Roquemore W.M., Role of inner and outer structures in transitional jet diffusion flame, *Combustion and Flame*, Vol.92, 1993, pp.274-282

[10] Yamashita, H., Idota, T. and Takeno, T., Effect of fuel on transition of fuel jet diffusion flame, *Trans JSME Ser. B*, Vol.62, 1996, pp.1226-1233